

Interferometric measurement of the vibrational characteristics of light-weight mirrors

James Millerd^{*a}, Mark Schmucker^a John Hayes^a Ron Eng^b, John Lassiter^b H. Philip Stahl^b, Ted Rogers^c,
James Hadaway^c and Joseph Geary^c

^a4D Technology Corporation, 3280 E. Hemisphere Loop, #112, Tucson AZ, USA 85706;

^bNASA Marshall Space Flight Center, Mail Stop SD73, Huntsville, AL 35812

^cUniversity of Alabama in Huntsville, 301 Sparkman Drive, Huntsville, AL 35899

ABSTRACT

We present a technique to characterize and quantitatively measure the vibrational mode shapes and amplitudes of mirrors concurrently with surface figure testing. The technique utilizes a fast interferometer that does not introduce any mass loading to the test structure. We present the fundamentals of the technique, discuss several modes of operation, such as resonant and transient response, and analyze the operational limits. The performance of the measurement system is characterized using a small ambient test mirror.

Keywords: Interferometry, vibration, surface measurement

1. INTRODUCTION

The use of light-weighted, multi-laminate, and segmented mirrors in large spaced-based telescopes and terrestrial adaptive optics systems can result in susceptibility to resonant vibrations. Although finite element models can be used to predict and dampen vibrational modes in these structures, it is desirable to verify actual modal performance prior to deployment. Because the mirror structures have very low density, placement of transducers, such as strain gauges or accelerometers, can cause significant mass loading and change the vibrational behavior of the structure, leading to erroneous results. Therefore, a non-contact optical method for characterizing lightweight mirrors is highly desirable.

Laser based vibration sensors (laser vibrometers) can measure single points with large frequency bandwidths (MHz) but require scanning to map a large structure and typically are not capable of determining the phase relationship between different spatial areas, unless multiple sensors are used simultaneously. In this paper, we present an interferometric technique that is capable of whole-field vibration measurement. The surface shape of the test article is measured in two states, and the shapes are subtracted to obtain the differential shape. The technique can be used on both specular and diffuse surfaces, although the laser power requirements for diffuse reflectors are significantly higher than for polished mirrors. We demonstrate the technique on moderate scale structures and show that both resonant and transient behavior can be studied.

2. MEASUREMENT TECHNIQUE

2.1 Simultaneous phase-shift measurement

The rapid surface shape measurement is accomplished with a spatial phase-shift interferometer where four phase-shifted interferograms are simultaneously generated on a single detector array.^{1,2} The optical layout of the interferometer, which is sold under the trade name of PhaseCam, is shown in Figure 1. The basic configuration of the interferometer is a Twyman-Green.³ A 1 mW, frequency stabilized, single mode helium-neon laser is used as the source. The laser is incident on a half-wave birefringent plate that is used to rotate the polarization angle. By rotating the polarization angle, the power split between the reference and test arms of the interferometer can be varied continuously.

^{*}james.millerd@4dtechnology.com; phone 1 520 294-5600; fax 1 520 294-5601; 4dtechnology.com

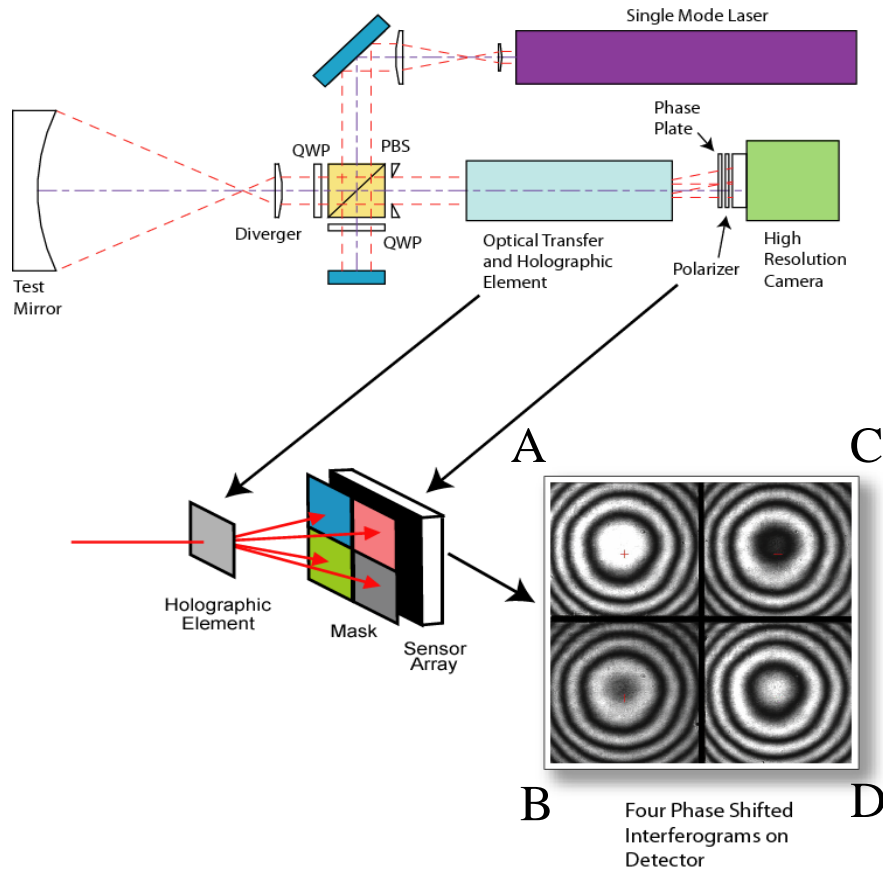


Figure 1. Layout of the simultaneous phase-shift interferometer (PhaseCam™).

The test arm of the interferometer is coupled to the test mirror either by a converging/diverging optic in the case of a convex/concave mirror, or is collimated by a telescope in the case of a plane mirror. The test and reference arms are recombined at the polarization beamsplitter and enter the imaging section. The imaging section splits the combined beams into four replicas and images the entrance pupil onto the detector. The entrance pupil position can be adjusted approximately 1 inch with a focus knob, located at the side of the interferometer. The four image replicas are transmitted through a polarization phase-mask, made from a combination of waveplates and polarizers, which is located just in front of the detector array. In this case, the detector array is a conventional CCD array having a resolution of 1000 x 1000 pixels. Each sub-image is approximately 500 x 500 pixels. Systems utilizing 4 million-pixel arrays, which have a sub-image size of 1000 x 1000, have also been demonstrated.

Because the four-interferograms are integrated at identically the same time, high accuracy measurements can be made in the presence of significant vibration in the test arm. With a 1 mW laser, 1M pixel CCD, and highly reflecting optics, the electronic integration time is on the order of 30 microseconds.

The shape of the mirror surface can be calculated from³

$$Z_{x,y}(t) = \frac{\lambda}{2} \operatorname{atan} \left(\frac{A_{x,y}(t) - C_{x,y}(t)}{D_{x,y}(t) - B_{x,y}(t)} \right) - Z_{system} \quad (1.)$$

where A, B, C and D are the intensities measured in each of the four sub-images and correspond to the relative phase-shifts of 0, 180, 90 and 270, respectively, and Z_{system} is the residual wavefront error in the system, which can be measured using a calibrated optical reference surface. The arctangent function results in a modulo 2π phase encoding, which must be removed by phase unwrapping techniques.⁴ We have demonstrated measurement of mirror surface

figures under cryogenic conditions with repeatability and accuracy better than 0.001 waves rms and 0.002 waves rms, respectively, by averaging 16 single measurements.⁵

2.2 Surface Subtraction

The simultaneous phase-shift architecture of the PhaseCam permits rapid measurement of the surface shape for specular reflecting objects. By subtracting two surface measurements on a pixel-by-pixel basis, one taken at time $t=0$ (baseline) and the other at a later time, t , any change of the surface shape occurring during the time interval can be detected. This can be expressed as

$$\Delta Z = Z(t) - Z_0, \quad (2.)$$

where the spatial coordinates x, y have been dropped for clarity.

Alternatively, the change in surface can be calculated by combining the 4 phase-shifted intensity values from each of the two measurements according to

$$\Delta Z = \frac{\lambda}{2} \operatorname{atan} \left(\frac{[D_0 - B_0][A(t) - C(t)] - [A_0 - C_0][D(t) - B(t)]}{[A(t) - C(t)][A_0 - C_0] + [D_0 - B_0][D(t) - B(t)]} \right) \quad (3.)$$

where the spatial coordinates x, y have been dropped for clarity, $A_0 - D_0$ are the intensity measurements of the baseline and $A(t) - D(t)$. Again, the arctangent function results in a modulo 2π phase encoding, which must be removed by phase unwrapping techniques.⁴ This second method is advantageous because it can be used with both specular and diffuse reflecting surfaces, and both speed and robustness are increased because phase unwrapping is performed only once.

2.3 Resonant mode identification

We found that a fast method to identify resonant modes in a sample is to view the modulation index map over the sample while varying the excitation frequency. The modulation index at each pixel is calculated according to³

$$\gamma_{x,y}(t) = \frac{2\sqrt{(A_{x,y}(t) - C_{x,y}(t))^2 + (D_{x,y}(t) - B_{x,y}(t))^2}}{D_{x,y}(t) + B_{x,y}(t) + A_{x,y}(t) + C_{x,y}(t)}. \quad (4.)$$

A large amplitude drive signal and/or a long camera integration time must be used so that regions of the sample with high velocity cause a loss of contrast in the fringe pattern. The patterns that are generated are similar to the electronic recording of time-averaged holograms.⁶ After the resonant modes are found, they can be measured quantitatively using the phase-difference or surface subtraction method.

2.4 Synchronous Capture

The basic setup for measuring spherical mirrors is shown in Figure 2. The light from the interferometer is coupled to the test optic with diverging/converging optic. A digital-to-analog conversion board, located inside the computer, generates both a drive signal and a trigger signal for the camera.

For the capture of synchronous events, a periodic waveform is generated on the analog output. The signal can be either sinusoidal or a square wave. Several possibilities for capturing data using the synchronous mode are illustrated in Figure 3. The phase sweep consists of a single frequency, sinusoidal excitation signal, where the trigger signal is timed to be coincident at a particular phase of the sinusoid. Because the data is processed between trigger events, many periods of the excitation waveform may elapse between acquisition events. A closely related capture mode is the use of non-sinusoidal, arbitrary excitation waveform where the trigger is timed to be coincident with a particular position of the waveform. Because the arbitrary waveform can contain many frequencies, it is more accurate to characterize this method as a temporal sweep rather than a phase sweep.

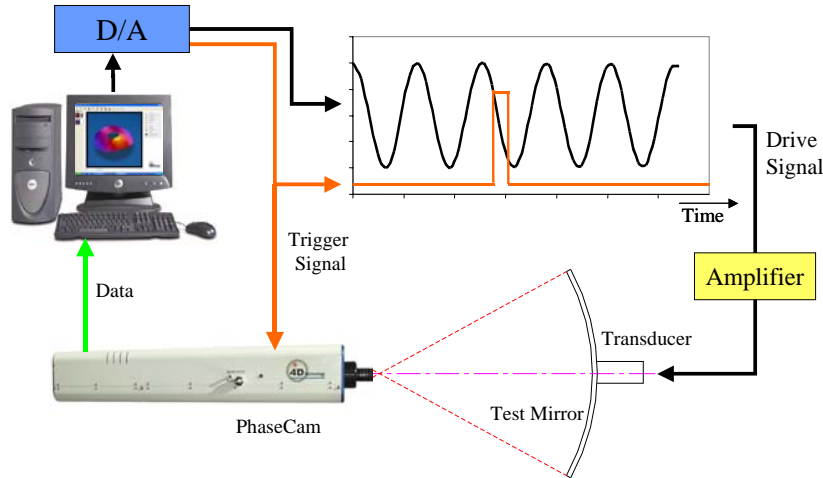


Figure 2. Conceptual layout of the measurement scheme.

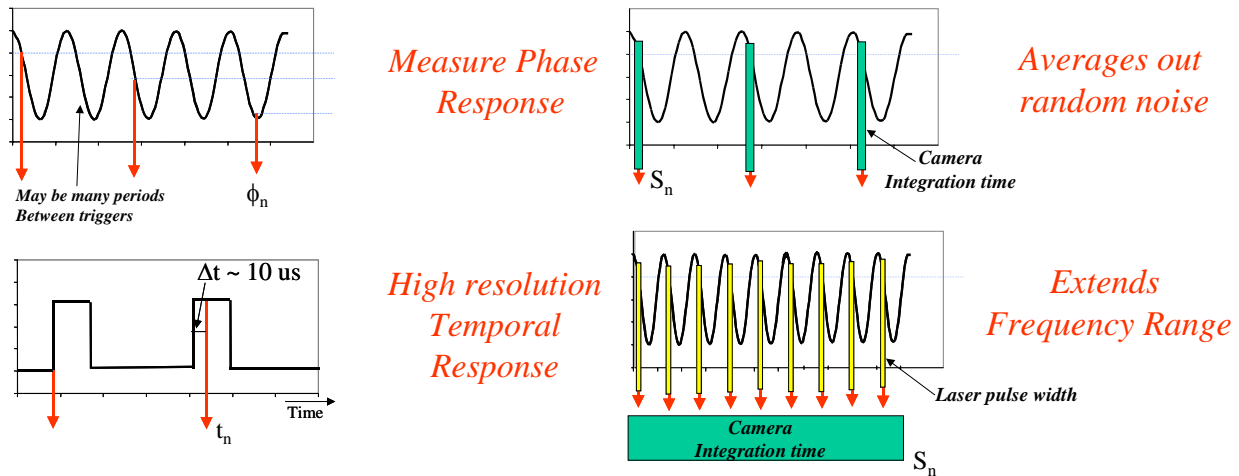


Figure 3. Synchronous capture modes. A) phase sweep, b) high resolution temporal sweep for transient response, c) averaging of multiple measurements at a constant phase to reduce noise and d) integrating multiple laser pulses to extend the frequency response range.

2.5 Averaging

Averaging mode can be used to reduce random noise or the contributions from modes other than the excitation frequency. The averaging process is shown in Figure 3c where multiple measurements are made at the same phase of the excitation signal and the resulting surface maps are averaged on a pixel-by-pixel basis.

A second form of averaging is shown in Figure 3d where short pulses of laser light are timed in phase with the driving signal. The purpose of this type of averaging is to extend the frequency response of the system. The extension of frequency response using pulsed laser light is discussed further in the next section.

2.6 Capture of Transient Events

For the capturing of transient events we capture data in a burst mode. A trigger event, which can be initiated internally through software or from an external event, initiates the capture of data. Data is acquired for a set time period and at a preset delay between each acquisition event. The analog output from the board can be used to trigger the transient excitation or to drive the excitation directly.

*james.millerd@4dtechnology.com; phone 1 520 294-5600; fax 1 520 294-5601; 4dtechnology.com

The frame rate of the camera and the data transfer from the frame grabber to the host limit the maximum capture rate. A standard 30 frame per second camera has a minimum time between samples of 33 milliseconds. Often the time between samples is slightly longer than this due to overhead in digitizing the signal and transferring to host memory. For a 1 million-pixel camera, burst measurements are recorded with approximately 50ms between each measurement.

2.7 Limits of Operation

Although the simultaneous interferogram phase-shift that occurs inside the PhaseCam makes the measurement possible, the integration time of the camera, or the laser pulse width, limits the vibrational velocity that can be measured. The displacement of the object should not be significant to an optical wavelength during the integration time and the oscillation period should be much greater than the integration time. For excitation at a single vibrational frequency, f , this relationship can be written as:

$$\int_t^{t+\tau} \Delta z_{\max} \cos(2\pi ft) dt \ll \frac{\lambda}{2} \quad \text{and} \quad \tau \ll \frac{1}{f} \quad (5)$$

where Δz is the maximum displacement at the point and λ is the optical wavelength. The maximum velocity at any one point on the sample is given by:

$$v_{\max} = \Delta z_{\max} \cdot f \quad (6.)$$

If the criterion for a good signal is set to a fringe contrast of 10%, the condition specified in equation 4 can then be written as

$$\Delta z_{\max} \cdot f \cdot \tau < \frac{\lambda}{4} \quad (7.)$$

Thus, for a given camera integration time, there is a maximum velocity or amplitude/frequency product that can be measured. For an integration times typical of camera electronic shutters (~30 microseconds) the maximum velocity that can be measured is approximately 1 mm/second, and a maximum frequency of approximately 8 kHz.

This range can be extended significantly by utilizing either a pulsed laser, which can have pulse durations of less than a nanosecond, or acousto-optic shutter and a CW laser source. Acousto-optic switching can generate pulses of less than a microsecond. Figure 4 shows the relation between maximum amplitude and frequency for the case of standard electronic integration, pulsed, and acousto-optic shutter. The maximum amplitude is bounded at low frequency by the maximum slope, or fringe density, that can be measured by the PhaseCam.

For the pulsed laser technique, the laser energy must be sufficient to generate the required signal on the CCD. The required energy can be estimated by considering that for a standard system measuring a high reflective mirror, integration times of 30 microseconds are sufficient with a 1 mW HeNe laser. Thus, approximately 0.03 microJoules per pulse is required. Additional losses in the system under test, such as low or diffuse reflectivity, can further increase the laser energy requirements.

For the acousto-optic modulation technique, it is possible to integrate multiple laser pulses during a single camera frame exposure so that a relatively low power source can be used. For a standard 1 mW laser, the overall integration time is simply increased by the modulator duty cycle. For example to measure a 100kHz signal, using a modulator pulse with of 1 microsecond the duty cycle is 10:1. Thus, the overall camera exposure is increased 10 times to 300 microseconds. Using a laser with higher power can reduce this further.

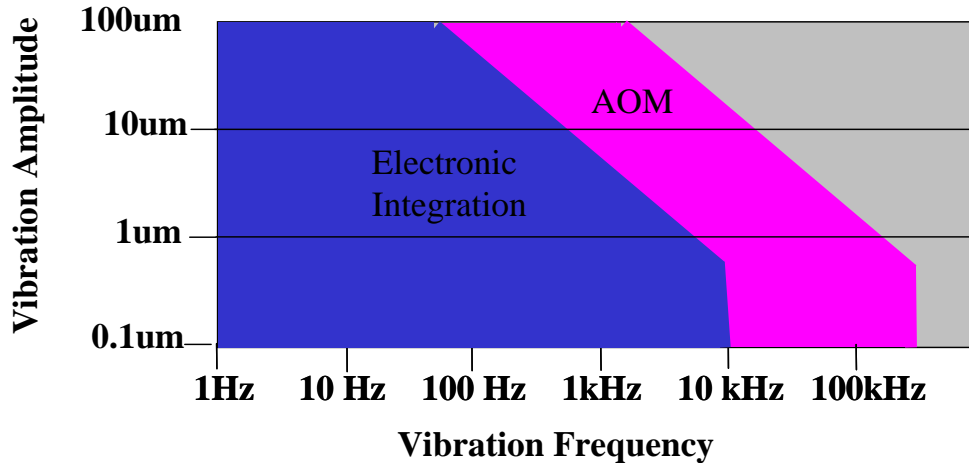


Figure 4. Maximum vibrational amplitude vs. vibration frequency for the two cases of a) electronic camera shutter and b) acousto-optic modulated laser shutter.

3. TEST RESULTS

3.1 Test article

To demonstrate the measurement system, we utilized a 95 mm diameter x 0.7 mm thick aluminum disk as our light-weight mirror. The disk was polished flat and had a hole in the center 15 mm diameter. The test mirror was mounted to a piezo-electric transducer stack with a small screw that was clamped at the top of the inner radius. The piezo stack was driven directly with the output from a PCI digital to analog conversion card. The test setup is shown in Figure 5. Special software was developed to synchronize the timing of the driving waveform with the camera trigger and to permit the phase, frequency and amplitude to be swept.

The nominal 7mm beam from the PhaseCam was focused and then expanded using a 60 mm focal length achromatic lens. The expanding light was collimated by a 150mm diameter, 600 mm focal length achromatic lens. The collimated light was reflected by the test mirror which was placed approximately 50 mm in front of the collimation lens. The focusing of the PhaseCam was adjusted so that the image of the disk through the telescope was at the entrance pupil.

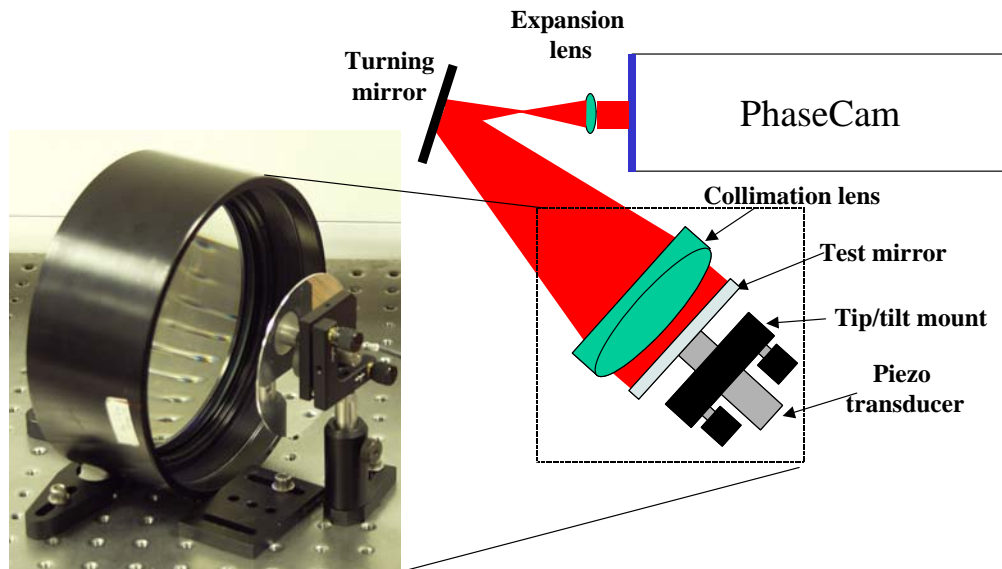


Figure 5. Optical layout of the test configuration and picture of the mirror assembly and collimation lens.

*james.millerd@4dtechnology.com; phone 1 520 294-5600; fax 1 520 294-5601; 4dtechnology.com

3.2 Static surface figure measurement

The test mirror had significant aberrations due to its small thickness and because of deformation caused by clamping it to the piezo-transducer stack. Figure 7 shows an interferogram of the surface and the resulting unwrapped surface profile. There were 20 waves of peak to valley deformation on the sample (equal to 12.6 microns).

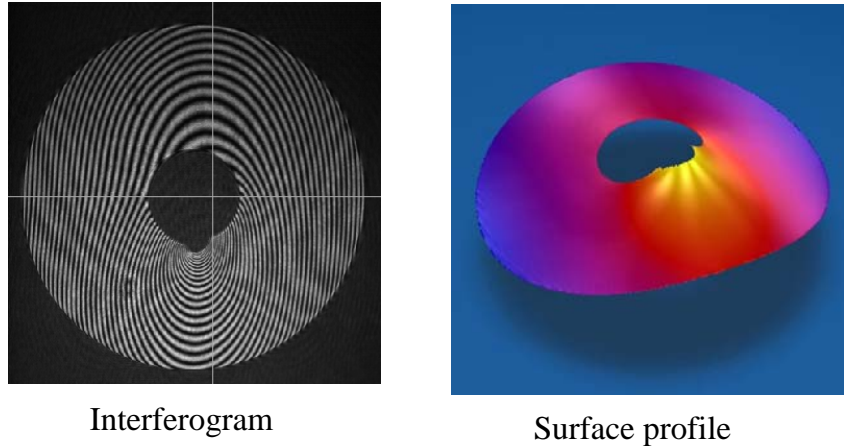


Figure 6. Measured surface figure for the static test mirror (peak to valley = 12.6 microns).

3.3 Resonant excitation

In the first series of tests we identified resonant modes by using a very high amplitude signal and observing a plot of surface modulation index. Resonant modes were quickly identified as a spatial pattern of reduced modulation across the sample. After noting the modes, we subsequently recorded a baseline image (t=0) without applying a drive signal to the piezo-electric stack and then subtracted measurements made at the resonant frequency. Several of the modes measured are presented in Figure 7.

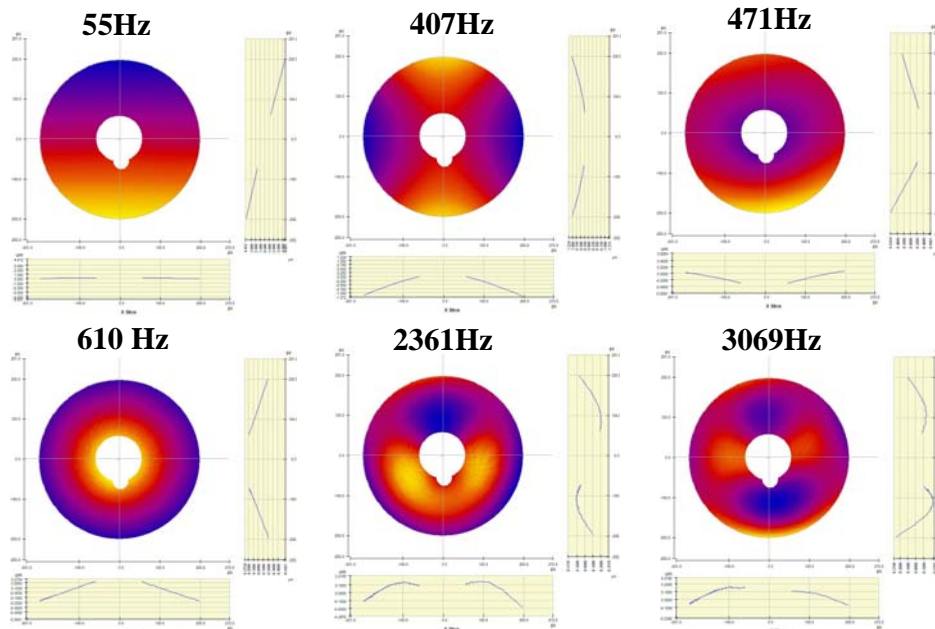


Figure 7. Several vibrational modes measured for the test mirror.

In a second set of experiments, we focused on the resonant mode at 408 Hz to demonstrate the sweeping of phase. We stepped the phase 22 degrees between each measurement. Every other measurement is plotted in Figure 8. Because the test setup was relatively stable, we only recorded one measurement at each phase increment and did not utilize averaging.

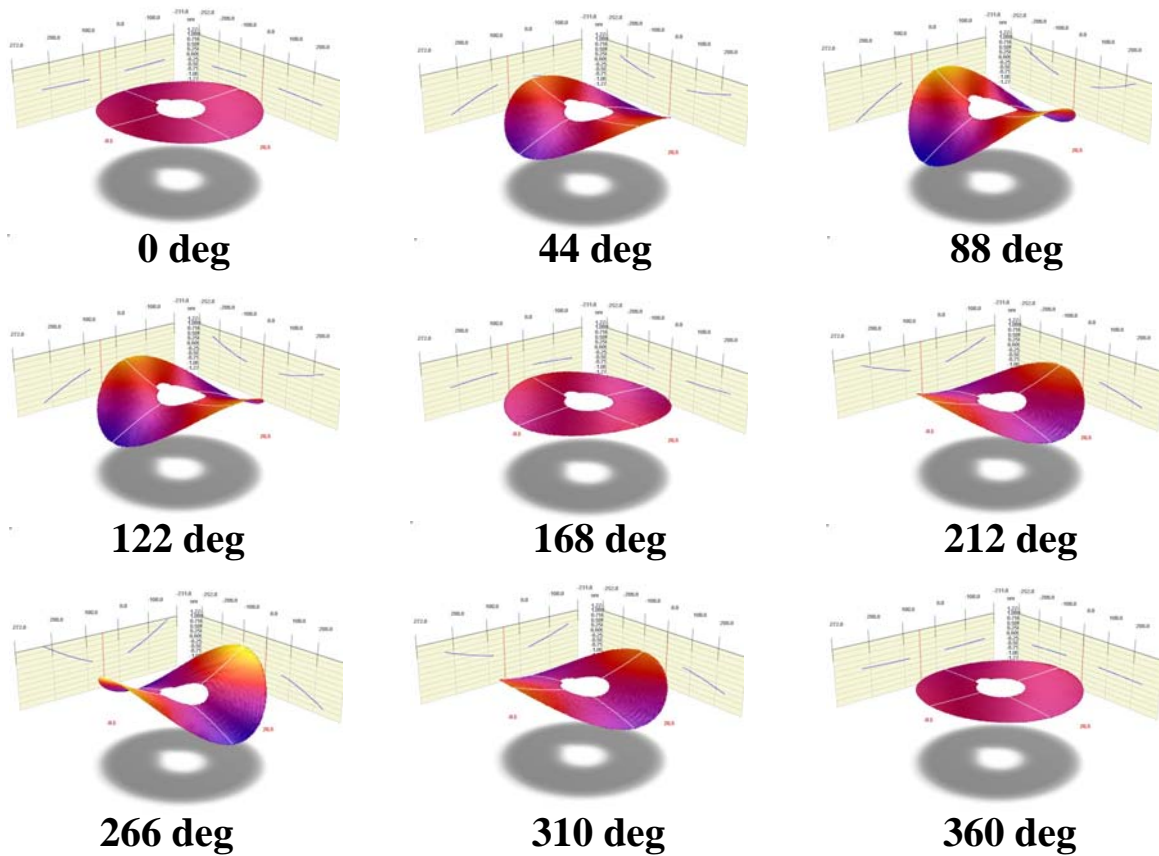


Figure 8. Sweep of phase through a resonant mode at 408 Hz.

3.4 Parameter sweeps

A useful tool for finding resonant modes is to vary the frequency and phase of the drive signal and record the amplitude of the deformation (either peak to valley or rms across the whole surface). For large parameter ranges, the majority of the data will not be at a resonant mode, so it is more convenient to simply record the rms and PV numbers and not save the actual surface maps. It was found that a useful metric for evaluating the relative vibrational magnitude is to plot the rms amplitude squared. Physically this quantity is proportional to the power in the mode and provides a better rejection of background vibrational noise that may be present. To demonstrate the ability to use multi-parameter sweeps, we scanned around a resonance at 510 Hz with 1Hz frequency steps and at each of 4 phases (0, 90, 180, 270). The results of the scan are shown in Figure 9.

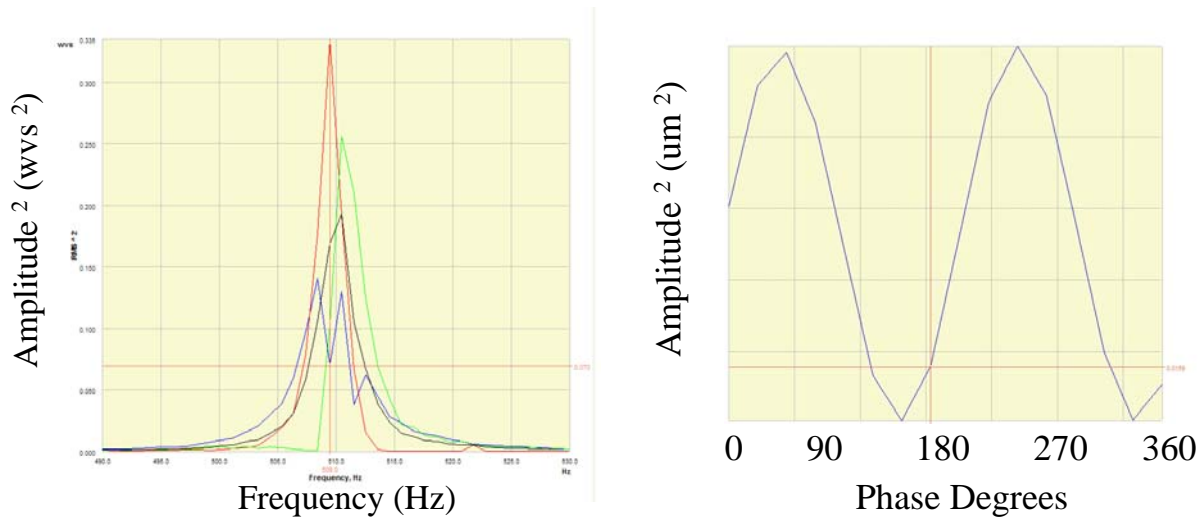


Figure 9. a) Sweep of frequency near a resonant mode for several discrete phase values, b) sweep of phase at a 408Hz resonant mode.

4. SUMMARY

We have presented a technique that is suitable for measuring resonant and transient vibrational characteristics of light-weight mirror structures. The non-contact measurement can be performed on both polished and unpolished optics, although the laser power requirements for large unpolished optics can be significant. For polished optics, measurements can be made with a low-power laser up to 8 kHz, and up to 100kHz for modest power lasers (30 mW). Custom software tools permit the rapid acquisition and playback of phase or temporal “movies” that allow easy visualization of the structural deformation as well as quantitative measurement. Multi-parameter sweeps in phase, frequency, and/or amplitude can reveal a wealth of information about the structural dynamics of the test article.

REFERENCES

1. A. Hettwer, J. Kranz, J. Schwider, “Three channel phase-shifting interferometer using polarization-optics and a diffraction grating,” *Optical Engineering*, pp 960, Vol. 39 No. 4, April 2000.
2. J. E. Millerd and N. J. Brock, US Patent No. 6,304,330 “*Methods and Apparatus for splitting imaging and measuring wavefronts in interferometry*,” Oct 16, 2001
3. Interferogram Analysis for Optical Testing, Malacara, Servin, and Malacara, Marcel Decker, Inc., New York, 1998
4. Two-dimensional Phase Unwrapping. Theory, Algorithms and Software, Ghiglia and Pritt, Wiley Interscience, New York, 1998.
5. J. E. Millerd, N. J. Brock, J. W. Baer, and P. Spuhler, “Vibration insensitive, interferometric measurements of mirror surface figures under cryogenic conditions,” Paper 4842-41, SPIE Proceedings, Specialized Optical Developments in Astronomy, August 2002.
6. R. J. Pryputniewicz and K. A. Stetson, “Measurement of vibration patterns using electro-optic holography” *Laser Interferometry: Quantative Analysis of Interferograms*, Proc. SPIE Vol 1162 pp. 456-467 (1989)